Frontiers in Bioscience Landmark

Front. Biosci. (Landmark Ed) **2022**; 27(1): 018
http://doi.org/10.31083/j.fbl2701018

Original Research

Screening a redox library identifies the anti-tumor drug Hinokitiol for treating intrahepatic cholangiocarcinoma

Peiying Bai[1,†], Chen Ge[1,†], Hui Yang[2,3,†], Haixu Chen[4,†], Lingfei Wan[1], Yuchen Zhang[1], Biao Zhang[2], Quan Zeng[2], Zeng Fan[2], Xuetao Pei[2,*], Wen Yue[2,*], Xinlong Yan[1,*]

[1]Faculty of Environmental and Life Sciences, Beijing University of Technology, 100124 Beijing, China
[2]Stem Cell and Regenerative Medicine Lab, Institute of Health Service and Transfusion Medicine, AMMS, 00850 Beijing, China
[3]Academy of Military Medical Sciences (AMMS), Academy of Military Sciences, 100071 Beijing, China
[4]The Second Medical Center, Chinese PLA General Hospital, 100853 Beijing, China
*Correspondence: Yxlong2000@bjut.edu.cn (Xinlong Yan); Yuewen0206@126.com (Wen Yue); Peixt@nic.bmi.ac.cn (Xuetao Pei)
†These authors contributed equally.
Academic Editor: Graham Pawelec
Submitted: 28 August 2021 Revised: 4 December 2021 Accepted: 7 December 2021 Published: 13 January 2022

Abstract

Aims: Intrahepatic cholangiocarcinoma (ICC) is a highly malignant and heterogeneous cancer with a poor prognosis. At present, there is no optimal treatment except for surgical resection, and recurrence after resection will lead to death due to multidrug resistance. Changes in the redox signal have been found to be closely related to the growth and drug resistance of tumor cells. Therefore, the purpose of this study was to screen small molecule compounds from the redox library to find a drug for anti-ICC and to explore its downstream mechanism. **Material and methods**: Tumor clone and sphere formation of ICC cell lines, as well as mouse ICC organoid proliferation assays were utilized to screen the candidate drug in the Redox library. Western blotting, quantitative reverse-transcription polymerase chain reaction (qRT-PCR), as well as cell apoptosis and cell cycle flow cytometry assays were used to explore the mechanism. **Results**: We found that Hinokitiol was a candidate drug through inhibition of tumor clone and sphere formation, and the expression of cancer stem cell (CSC)-related genes. Furthermore, Hinokitiol significantly inhibited the proliferation of ICC cells by downregulating the ERK and P38 pathways. In addition, the combination of Hinokitiol and Palbociclib showed a significant inhibitory effect on human ICC cells and mouse ICC organoids. **Conclusion**: Hinokitiol may have the potential to be developed as a clinical therapeutic drug for ICC treatment.

Keywords: Redox library; Intrahepatic cholangiocarcinoma; Hinokitiol; Proliferation; Tumor sphere; Tumor organoids

1. Introduction

Intrahepatic cholangiocarcinoma (ICC), which originates from intrahepatic bile duct epithelial cells, is the second most common human primary liver cancer after hepatocellular carcinoma (HCC) [1,2]. Recently, studies have shown an increasing incidence and mortality rate of ICC, especially in Eastern Asia [3]. Although surgical resection is the most effective treatment for early stage ICC, only a few patients are suitable for this therapy [4,5], as the majority of ICC patients are diagnosed at an advanced stage, lacking the opportunity for resection [6], and recurrence leading to multidrug resistance is the key problem of ICC treatment [7,8]; therefore, it is essential to develop a chemotherapy regimen to overcome this refractory malignancy.

Redox signaling has been reported to be a feasible target for overcoming multidrug resistance in cancer chemotherapy [9,10]. Changes in the oxidation-reduction equilibrium state may lead to oxidative stress and abnormal cell signal transduction [11,12], which in turn regulate redox-sensitive enzymes and transcription factors [13]. It can also directly affect the curative effect of cancer treatment through various mechanisms, such as apoptosis, growth inhibition [14], angiogenesis, and metastasis [15,16]. For example, higher ROS levels could promote the development of cancer by inducing DNA mutations [17,18], genome destruction, and abnormal signal transduction of tumor initiation, proliferation, and drug resistance [19]. Detoxifying enzymes and antioxidant proteins in redox-related pathways play a key role in regulating the balance between apoptosis and carcinogenesis [20]. Moreover, the overactivation of nuclear factor-erythroid 2 related factor 2 (Nrf2), a redox-sensitive factor, may be involved in the occurrence of breast cancer and ovarian cancers [21,22]. Apurinic-apyrimidinic endonuclease 1/redox factor 1 (APE-1/Ref-1) [23], another redox factor, can promote the binding of transcription factors to gene promoters involved in cancer initiation and progression. These redox-related factors may be responsible for the occurrence and development of tumors. Therefore, regulating the redox levels of tumor cells may be of great significance for the development of potential anti-cancer therapies.

The redox library in our study contains a variety of 84 small molecular chemical compounds that inhibit the redox reaction. In this study, we explored whether these small molecules in the redox library can effectively inhibit the clone formation and tumor sphere formation in ICC cells.

We screened the redox library and found that #15 Hinokitiol was the candidate molecule that could inhibit the cancer stemness of ICC cells. Using qRT-PCR assays, flow cytometry, and western blotting analysis, we found that some CSC-related markers were downregulated by #15 Hinokitiol treatment through inhibition of the ERK and P38 pathways. Based on the functional role of Hinokitiol in the repression of proliferation and tumor sphere formation of ICC cells, Hinokitiol has the potential to develop into a new anticancer drug with good biological safety.

2. Materials and methods

2.1 ICC cell culture, redox library and animals

All animal experiments in this study were conducted in accordance with ethical regulations and approved by the Ethics Committee of the Academy of Military Medical Sciences.

Intrahepatic cholangiocarcinoma cell line HuCCT1 cell was provided from Beijing Beina Chuanglian Biotechnology Institute. RBE and HCCC-9810 cell lines were obtained by China Infrastructure of Cell Line Resource (CICR). QBC939 cell line was given by Prof Jiahong Dong (Beijing Tsinghua Chang Gung Hospital, Beijing, China). ICC cell lines (QBC939 and HuCCT1) were grown in high glucose DMEM medium supplemented with 10% FBS (Invitrogen), 100 μg/mL penicillin, and 100 U/mL streptomycin. RBE and HCCC-9810 cells were cultured in RPMI1640 medium supplemented with 10% FBS, 100 μg/mL penicillin, and 100 U/mL streptomycin at 37 °C under 5% CO_2.

Redox library was established from Center for Excellence in Molecular Cell Science, Chinese Academy of Sciences (Shanghai, China), as shown in **Supplementary Table 1**. All the small molecular drugs were dissolved in DMSO and the storage concentration was 10 mM.

2.2 Clone formation assays

A total of 1500 ICC cells were seeded in the 24-well plates (Corning, USA) and cultured in the DMEM medium supplemented with 10% FBS (Invitrogen). After 24 h, ICC cells were treated with 84 small molecules in the redox library with a concentration of 10 μM for 7 days. The ICC clones were fixed with 4% paraformaldehyde and stained with 0.25% crystal violet at room temperature (RT) for 30 min, then washed with PBS, the clones over 50 cells were counted under stereomicroscope.

2.3 Tumor sphere formation assays

A total of 3000 ICC cells were seeded in the 6-well ultra-low attachment plates (Corning, USA) and cultured in the DMEM/F-12 supplemented with B27 (Life Technologies, USA, 1:50), N2 (Life Technologies, 1:100), 20 ng/mL epidermal growth factor (EGF), 10 ng/mL bFGF, 100 units/mL penicillin, and 100 ng/mL streptomycin and seven preliminary screening small molecules with a concentration of 10 μM for 5 days. Tumor spheres larger than 100 μm were observed and recorded by microscope.

2.4 Immunohistochemistry

Paraffin-embedded tissue sections were dewaxed and hydrated in alcohol, then, 10% hydrogen peroxide was added for 30 min to remove endogenous peroxidase. After induction of Antigen epitope retrieval by microwave heating. Tissues were immunostained with primary antibodies overnight at 4 °C. The secondary antibody used for immunostaining was biotin-conjugated anti-rabbit immunoglobulin (Beijing Zhongshan Biotechnology). The immunodetection was performed on the following day using an PV-9001 kit (Beijing Zhongshan Biotechnology) according to the manufacturer's instructions. Hematoxlin was used for counterstaining. The antibodies were listed in **Supplementary Table 2**.

2.5 Cell apoptosis assay and cell cycle analysis

The cell apoptosis was detected with Annexin V, FITC Apoptosis Detection Kit (Dojindo, #AD10-10). A total of 2×10^5 ICC cells per well were seeded in 6-well plates, and 24 h later, the medium was replaced with 3 mL DMEM medium containing Hinokitiol followed by 48 h incubating, and then the ICC cells were detached with EDTA-free trypsin and suspended in 1$\times$ Annexin V Binding solution, then added 5 μL Annexin V- FITC and incubated at RT for 15 min, 400 μL PBS was added to stop the reaction, then the cells were analyzed by flow cytometry assays.

A total of 1×10^6 ICC cells were treated by 3 mL DMEM medium containing Hinokitiol. After treatment for 48 hours, the cells were collected and fixed in 75% ethanol solution over 4 hours. The cells were centrifuged (400 $\times$ *g*, 5 min) and washed with PBS twice, and suspended at 10^6 cells/mL. 20 μg/mL of RNase A was added to each sample and incubated at 37 °C for 30 min. Then 20 μg of propidium iodide was added to each tube for 15 min protected from light. The distribution of cells in each phase of the cell cycle were analyzed by flow cytometry analysis.

2.6 Quantitative reverse-transcription polymerase chain reaction analysis (qRT-PCR)

Total RNAs were extracted from the cells with TRIzol (Invitrogen). The amount of RNA was quantified spectrophotometrically with a Nano-Drop ND-1000. Reverse transcription of total RNAs into cDNA was performed with a reverse transcriptase kit (FSQ-201, TOYOBO, Japan). The relative mRNA expression was determined by real time PCR using THUNDERBIRD SYBR qPCR Mix (QPS-201, TOYOBO, Japan). Briefly, a 20 μL qPCR system was performed for 40 cycles according to the following conditions: An initial denaturation was performed at 95 °C for 3 min, followed by denaturation at 95 °C for 15 sec, annealing at 58 °C for 30 sec, and extension at 72 °C for 7 min. Relative quantification of mRNA expression was calculated us-

ing the $2^{-\Delta\Delta Cq}$ method. 18S was used as a housekeeping gene. The mRNA primer sequences were list in **Supplementary Table 3**.

2.7 Western blotting

The ICC cells were lysed with RIPA buffer (50 mM Tris-HCl, pH 7.5, 150 mM NaCl, 1% NP-40, 0.5% sodium deoxycholate, 0.1% SDS) supplemented with protease inhibitors (Calbiochem, San Diego, California), and equal amounts of protein was separated by SDS-PAGE (10% polyacrylamide), and then transferred the protein to polyvinylidene difluoride membranes (PVDF, BioRad, Hercules, CA). The membranes were incubated with primary antibody overnight at 4 °C after blocking in TBST containing 5% skimmed milk. The membrane was washed three times with TBST, and then incubated with horseradish peroxidase-bound secondary antibody (Beijing Zhongshan Biotechnology Co., Ltd., Beijing, China) for 1 h at RT. After washing three times with TBST, the immunoreactive band was detected by enhanced chemiluminescence method (Santa Cruz Biotechnology Company, Santa Cruz, California), and then exposed with BioMax film (Kodak Company, Rochester, New York) according to Clarity Max™ Western ECL Substrate (Bio-Rad, USA). The antibody information is listed in **Supplementary Table 3**.

2.8 Mouse ICC model and isolation of primary mouse ICC cells

C57BL/6 mice of 8~10 week old were purchased from Vitalriver (Beijing, China) and raised under specific pathogen-free conditions. The plasmids ddAKT and ddYAP were kindly gifted by Prof Yuji Nishikawa (Asahikawa Medical University, Asahikawa, Hokkaido, Japan). The plasmid containing Sleeping Beauty transposon (SB13) was preserved in the laboratory. These three plasmids were dissolved in 2 mL saline and injected into the mouse via tail vein injection (5~7 s). After 8~10 weeks, the abdominal bulge was observed and the mice were euthanized. The tumor tissue (about 3~5 mm^3) was cut with surgical scissors under the aseptic condition. Then the ICC tissue fragments were washed with PBS twice. After centrifugation at 400 $\times$ *g* for 5 minutes, tumor fragments were dissociated into single cells under 20 mL mouse Tumor Dissociation Kit (Miltenyi Biotec, #130-096-730) within 1h at 37 °C. After dissociation, cells were filtered through a 70 μm cell strainer (BD Falcon, #352350). The primary tumor cells were treated by ACK Lysing Buffer (Gibco, #A1049201) for 3 minutes and were harvested after centrifugation at 500 $\times$ *g* for 5 minutes at 4 °C.

2.9 Mouse ICC organoid culture

Isolated primary mouse ICC cells were dissolved in the organoid culture medium (Stemcell, #06030) and mixed with Matrigel (BD, #356234) in precooled EP tube and and suspended the pellet at 4 °C. Add 150 μL matrigel to 150 μL suspension in a 1.5 mL tube and mix cells to avoid bubbles. About 20000 cells in 50 μL suspension was used per well of the preheat 24-well plate. After Matrigel was solidified for 15 min, 500 uL mouse organoid culture medium was added. After seeding for 7~14 days, organoids were mechanically fragmented and re-seeded into new Matrigel or cryopreserved in liquid nitrogen. Rho-associated protein kinase (ROCK) inhibitor Y27632 was added to the culture medium additionally after 3–4 days. Then, Hinokitiol with a concentration of 4 μM, Palbociclib with a concentration of 1 μM, and the combination of Hinokitiol and Palbociclib were added in the culture medium. According to the growth rate of the ICC organoids, the passage was carried out in the ratio of 1:4. On the second day, the medium containing different drugs was added to tumor organoids. The results were observed and photographed in 3~10 days.

2.10 Statistical analysis

We analysed the data using GraphPad Prism software version 8 (GraphPad Software, San Diego, California, US). Comparisons between two groups were performed with unpaired *t* tests. All experiments were conducted at least three times and data are presented as means $\pm$ standard deviations (SDs). N.S. means no significantly difference, $*p < 0.05$, $**p < 0.01$, $***p < 0.001$.

3. Results

3.1 Preliminary screening of redox library by tumor clone formation assays

The anti-tumor effect of 84 different small molecules in the redox library with four human ICC cell lines were preliminary screening using clone formation assays (Fig. 1A–D). The representative clone formation of preliminarily screened four ICC cell lines is displayed in Fig. 1E, **Supplementary Fig. 1A–C**. We statistically analyzed and merged the inhibitory effect on four ICC cell lines treated with 84 different small molecules in the redox library, as shown in Fig. 1F. Eight small molecule inhibitors (#3, #15, #40, #54, #61, #67, #68, and #71) showed a significant decrease in clone formation capacity compared with the control group treated with DMSO. Among them, #54 (n-Octylcaffeate) has not been sold in China, so we will not consider using this drug for further exploration. These preliminary results indicated that these seven small molecule inhibitors could significantly suppress the proliferation of human ICC clones.

3.2 Screening of the candidate small molecules with tumor sphere formation assays

The tumor sphere formation assay is a standard method for evaluating the proliferation ability of CSCs *in vitro*. The above seven candidate small molecular inhibitors were further screened for their effects on tumor sphere formation in four human ICC cell lines (Fig. 2A–E, **Supplementary Fig. 2A–C**). The number of tumor spheres treated by these candidate small molecules was

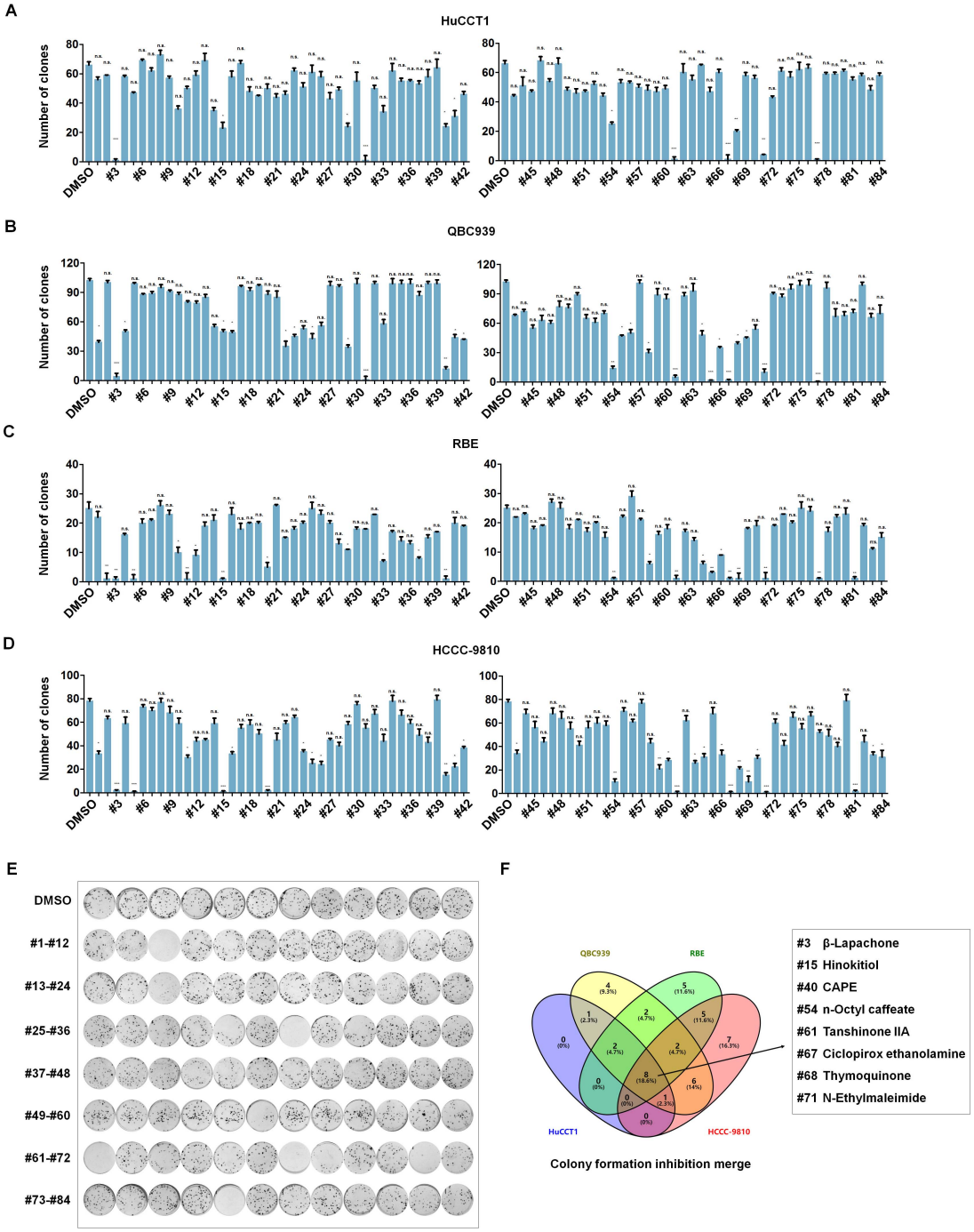

Fig. 1. Preliminary screening of drugs from the redox library via clone formation assays. (A–D) The column graph of HuCCT1 (A), QBC939 (B), RBE (C), and HCCC-9810 (D), each treated with small molecules in the redox library, compared with the control group. (E) Photos of the clone formation assay of HuCCT1 cells treated with various drugs in the redox library. (F) Venn diagram of anticancer drugs (with over 50% anti-tumor effect) in four ICC cell lines treated with 84 drugs from the redox library. Data was analyzed using unpaired *t* test. N.S., no significance, $*p < 0.05$, $**p < 0.01$, $***p < 0.001$.

statistically analyzed using a column graph and Venn diagram (Fig. 2F). The results showed that β-Lapachone (#3), Hinokitiol (#15), Tanshinone IIA (#61), and Ciclopirox ethanolamine (#67) exerted a marked anti-proliferative effect on human ICC tumor sphere formation compared with other drugs.

3.3 Hinokitiol modulated the expression of CSC-related markers

Drug resistance caused by CSC enrichment has been proven to be the main cause of chemotherapy failure and

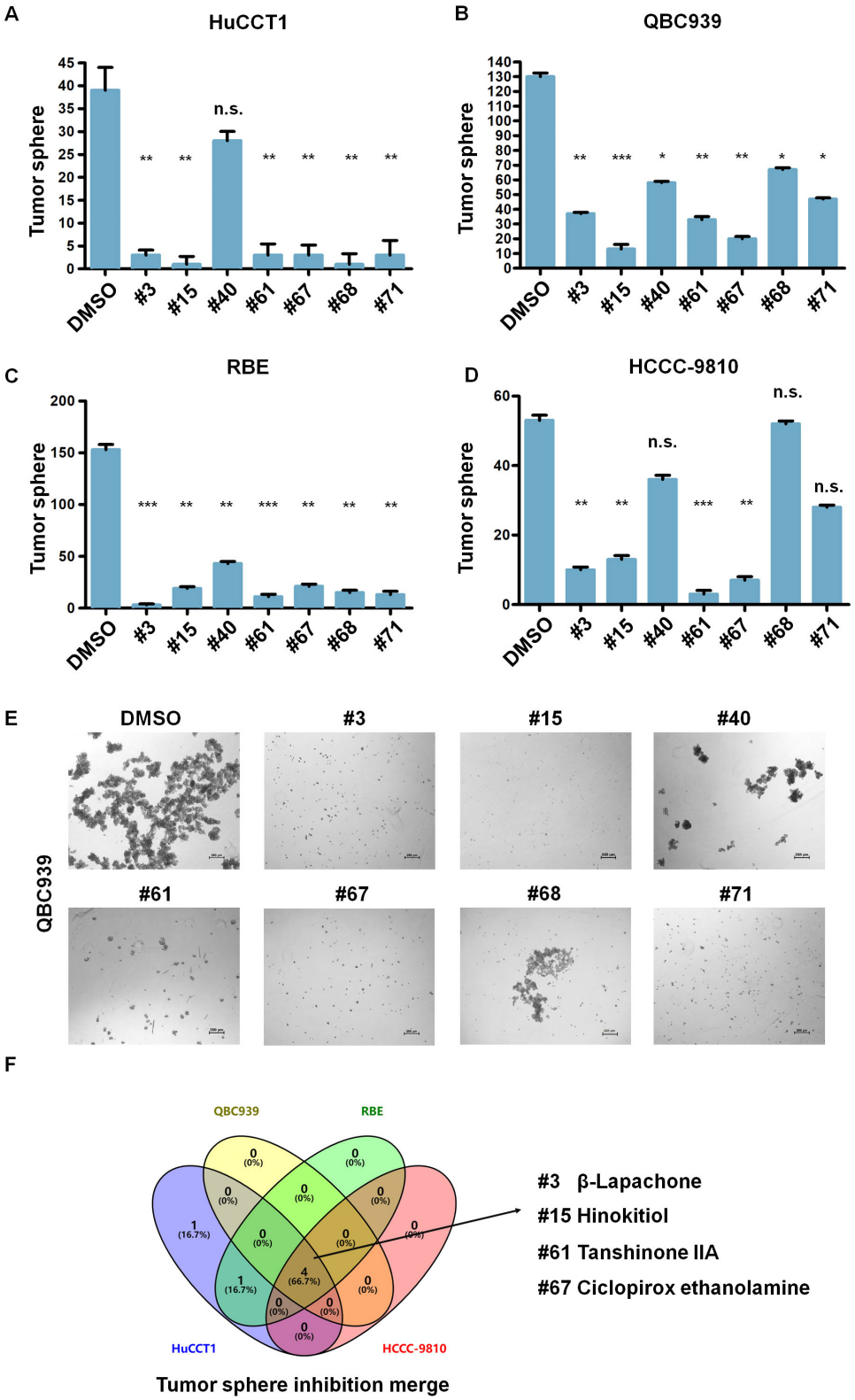

Fig. 2. Screening of drugs from the redox library via tumor sphere formation assays. (A–D) The column graph of the tumor sphere formation of HuCCT1 cells (A), QBC939 cells (B), RBE cells (C), and HCCC-9810 cells (D), each treated with small molecule compounds from redox library. (E) Photos of the tumor sphere formation in QBC939 cells treated with small molecules in the redox library; Scale bar = 250 μm. (F) Venn diagram of the tumor sphere analysis of four ICC cell lines treated with small molecules in the redox library. Data was analyzed using unpaired *t* test. N.S., no significance, *$p < 0.05$, **$p < 0.01$, ***$p < 0.001$.

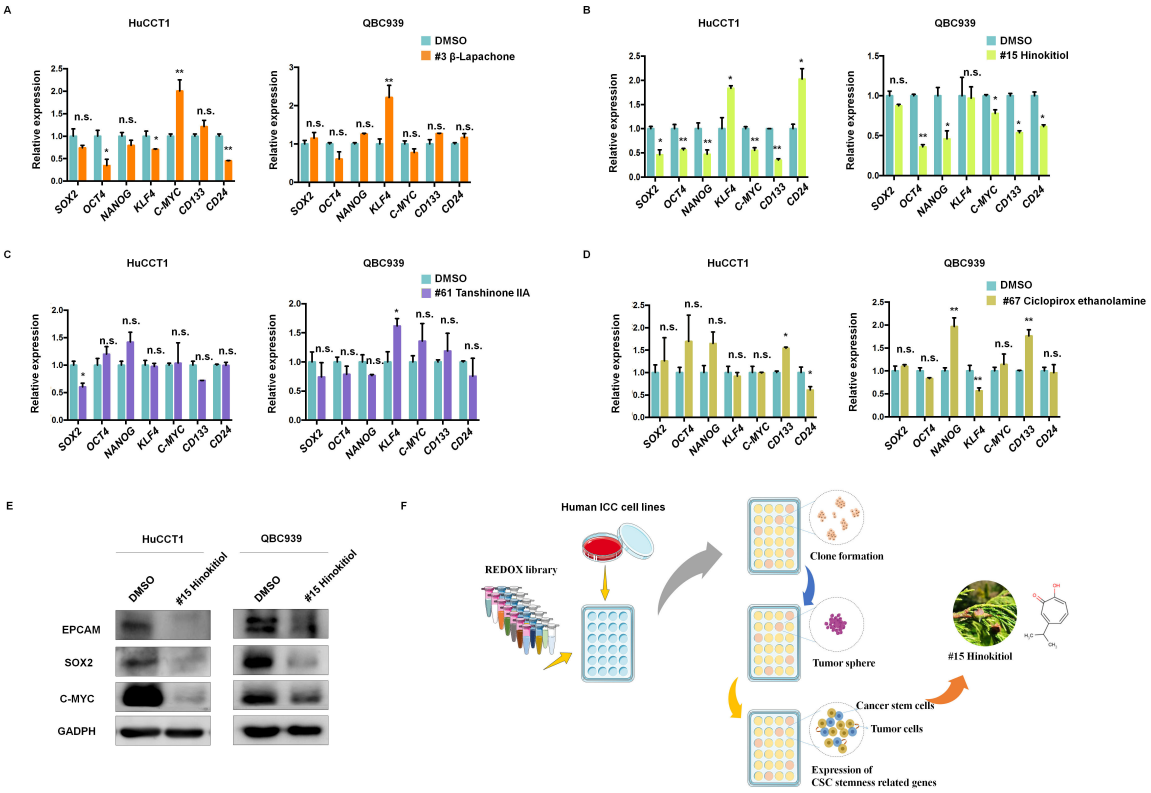

Fig. 3. Hinokitiol significantly inhibited some CSC-related markers. (A–D) Relative expression of CSC-related genes in HuCCT1 and QBC939 cells treated with β-Lapachone (A), Hinokitiol (B), Tanshinone IIA (C), and Ciclopirox ethanolamine (D). (E) Western blotting analysis of the CSC-related markers in HuCCT1 and QBC939 cells treated with DMSO or Hinokitiol, respectively. (F) Screening strategy of the redox library in human ICC cells. Data was analyzed using unpaired *t* test. N.S., no significance, $*p < 0.05$, $**p < 0.01$, $***p < 0.001$.

cancer recurrence in various cancers [24]. We detected the altered expression of CSC-related genes in human ICC cells treated with four candidate drugs at the secondary screening stage using qRT-PCR assays (Fig. 3A,B,C,D). Compared to the control group treated with DMSO, we found that several CSC-related markers, excluding *KLF4* and *CD24* in HuCCT1 and QBC939 cells, were significantly down-regulated by #15 Hinokitiol, not by #3 β-Lapachone, #61 Tanshinone IIA, and #67 Ciclopirox ethanolamine treatment. Moreover, western blotting analysis was used to detect the expression of CSC-related markers at the protein level. The expression of EpCAM, SOX2, and C-MYC was dramatically decreased in both ICC cell lines treated with Hinokitiol (Fig. 3E), indicating that Hinokitiol remarkably inhibited the CSC characteristics of ICC cells. Overall, by screening the redox library by clone formation assays, tumor sphere formation assays, and CSC-related marker repression, we found that Hinokitiol could be an effective small molecular inhibitor to repress ICC proliferation (Fig. 3F).

3.4 Hinokitiol significantly inhibited the pathways of ERK and P38 in human ICC cells

Energy-dependent drug efflux, cell cycle promotion, and apoptosis escape are usually related to the drug resistance in CSCs [24]. To explore the downstream mechanism of ICC cells treated with Hinokitiol, we performed apoptotic and cell cycle analysis of ICC cells after Hinokitiol treatment using flow cytometry. As shown in Fig. 4A,B, there were no significant differences in the early and late apoptotic cell populations between the Hinokitiol-treated group and control cells. The cell cycle analysis also showed that there were no significant differences between the Hinokitiol-treated group and the control group in G1, G2, and S phrase (Fig. 4C,D). These results suggest that the concentration of Hinokitiol used in our experiments can inhibit the proliferation of ICC cells and CSCs (**Supplementary Fig. 3A,B**), but not through apoptosis induction or cell cycle blockage.

To further investigate the underlying mechanism of Hinokitiol-induced CSC repression in human ICC cells, we detected the expression of key target genes in various signaling pathways by qRT-PCR assays, including WNT, Hedgehog, NOTCH, mitogen-activated pro-

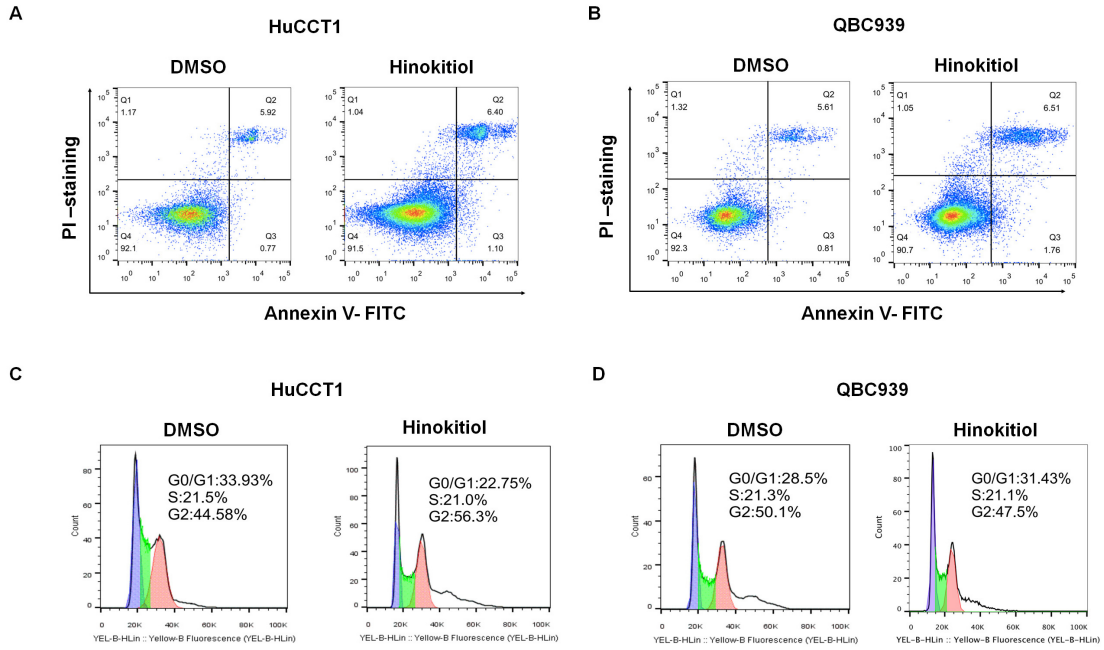

Fig. 4. Effects of Hinokitiol on the apoptosis and cell cycle of ICC cells. (A) Apoptosis of HuCCT1 cells treated with DMSO and Hinokitiol. Q1, Q2, Q3, and Q4 population represents the number of living cells, the number of late apoptotic cells, the error within the detection range, the number of early apoptotic cells, respectively. (B) Apoptosis of QBC939 cells treated with DMSO and Hinokitiol, respectively. (C,D) Cell cycle of HuCCT1 and QBC939 cells treated with DMSO and Hinokitiol, respectively.

tein kinase (MAPK), and epithelial-mesenchymal transition (EMT) (Fig. 5A,B). As shown in Fig. 5B, the expression of ERK2 and P38, which belong to the MAPK signaling pathway, exhibited a remarkable reduction in HuCCT1 and QBC939 cells in the Hinokitiol-treated group. Moreover, the expression levels of total and phosphorylated ERK and P38 proteins were further verified by western blot analysis (Fig. 5D). Overall, these results indicate that Hinokitiol may reduce the proliferation of human ICC cells by decreasing the expression of ERK, p-ERK, P38 and p-P38.

3.5 Hinokitiol combined with Palbociclib showed a significantly repressive effect of tumor sphere formation of human ICC cells

Human ICC is a malignant cancer with complex pathology and multiple targets. Combined drug therapy is becoming a trend in tumor treatment [25]. Cyclin-dependent kinase 4 and 6 (CDK4/6) is a promising target for ICC treatment, and Palbociclib, a CDK4/6 inhibitor, has been reported to synergize with pan-mTOR inhibitors to impair ICC growth [26]. As shown in Fig. 6A,B, combined Hinokitiol and Palbociclib treatment showed a much stronger anti-tumor effect than the single drug treatment in clone formation assays (Fig. 6A) and tumor sphere formation analyses (Fig. 6B). Overall, our results suggest that Hinokitiol combined with the CDK4/6 inhibitor Palbociclib could significantly inhibit the clone formation capacity and tumor sphere formation of human ICC cells.

3.6 Hinokitiol combined with Palbociclib significantly inhibited the formation of tumor organoids from mouse ICC models

3D tumor organoids derived from human primary tumor tissues and mouse tumor models are novel preclinical model systems that facilitate drug discovery and screening. The ICC mouse model was constructed by hydrodynamic transfection method [27,28] (Fig. 7A) and was verified by the immunohistochemical staining of CK19 (Fig. 7B). Thereafter, mouse primary ICC cells were purified from the induced mouse ICC tumor tissues and then cultured the mouse ICC organoids in three-dimensional (3D) medium, treated with Hinokitiol, Palbociclib, or combined drug, respectively (Fig. 7C,D). These results indicated that Hinokitiol exerted anti-tumor effects in mouse ICC organoids *in vitro*. In addition, Hinokitiol combined with Palbociclib significantly inhibited the formation of mouse ICC organoids.

4. Discussion

In the past 30 years, the incidence and mortality of intrahepatic cholangiocarcinoma have increased worldwide; however, only a few early stage patients can benefit from surgical resection, and most patients diagnosed at an advanced stage have to be treated with standard chemotherapy of platinum or cisplatin combined with gemcitabine; however, the combination treatment of these advanced state patients results in a poor prognosis, with only a median overall survival of 11 months [29]. Therefore, new treatments

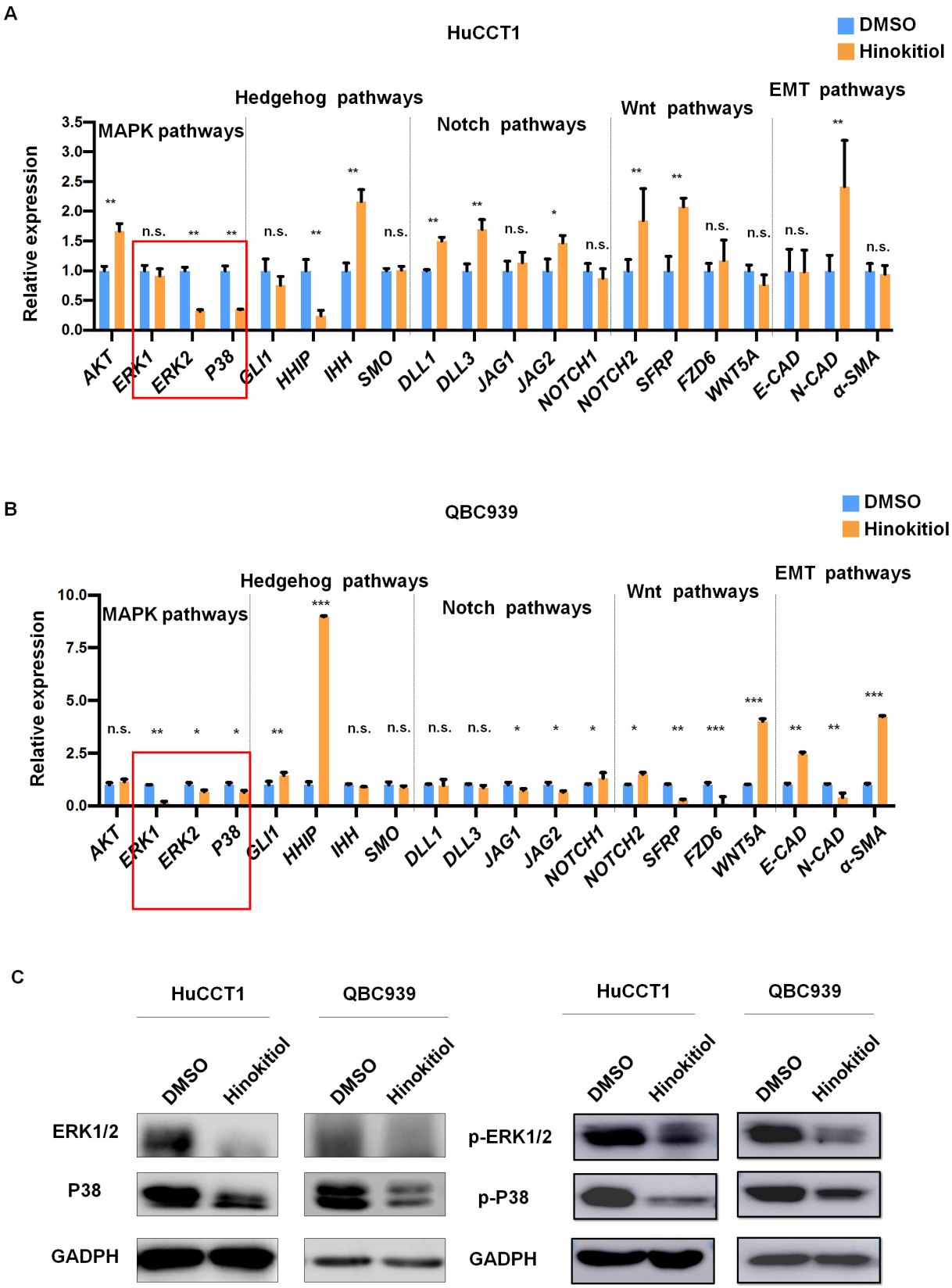

Fig. 5. Hinokitiol down-regulated the expression of ERK and P38 pathway of human ICC cells. (A,B) Various signaling pathways were detected by qRT-PCR technology in HuCCT1 (A) and QBC939 (B). (C) Western blotting assays of ERK1/2, p-ERK, P38 and p-P38 protein expression in HuCCT1 and QBC939 cells treated with Hinokitiol. Data was analyzed using unpaired *t* test. N.S., no significance, $*p < 0.05$, $**p < 0.01$, $***p < 0.001$.

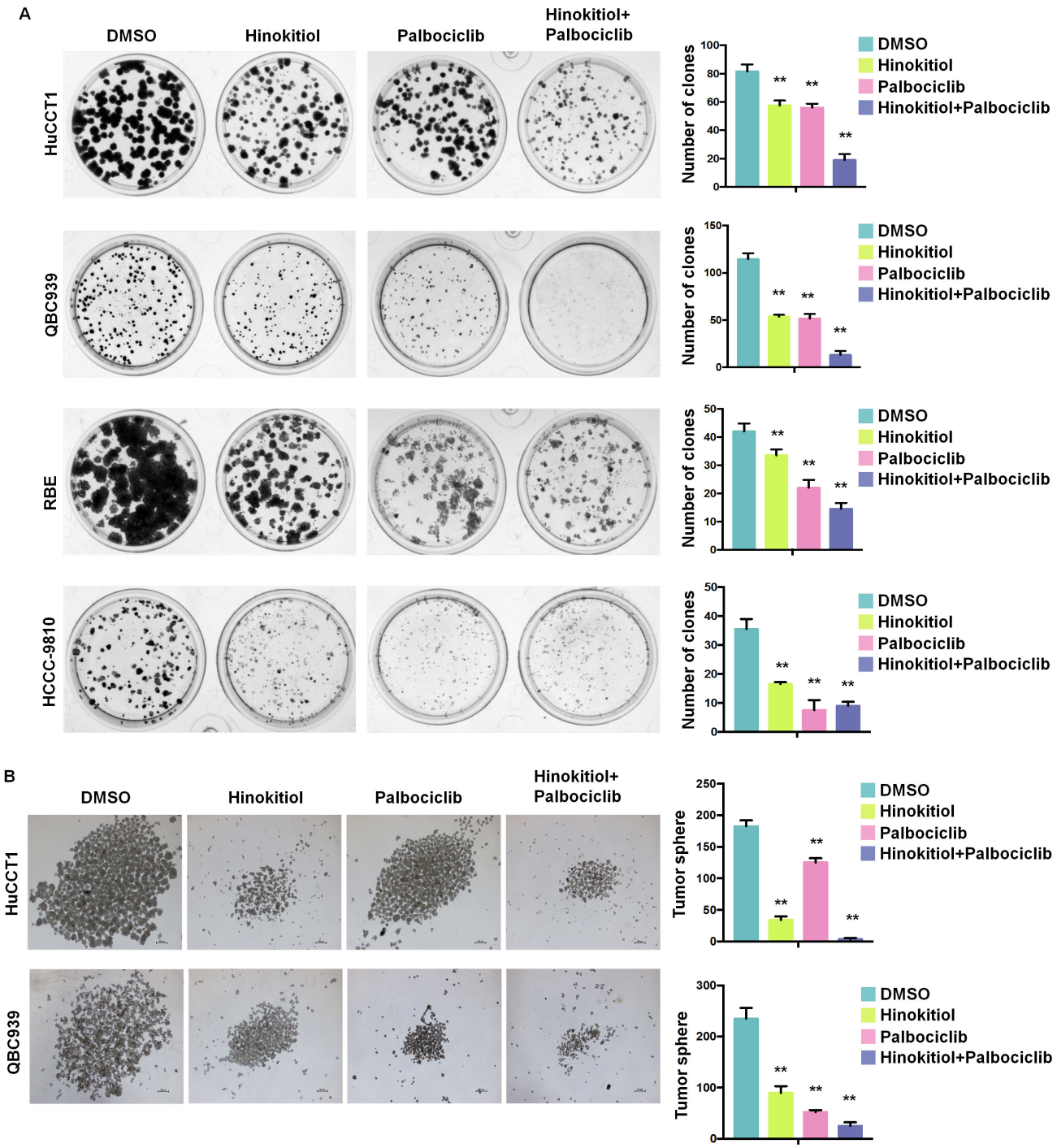

Fig. 6. Hinokitiol combined with Palbociclib significantly inhibited tumor sphere formation of human ICC cells. (A) The effects of Hinokitiol, Palbociclib, and combined group treatments were evaluated through clone formation assays in ICC cells. (B) The effects of Hinokitiol alone, Palbociclib alone, and Hinokitiol + Palbociclib treatments were evaluated by tumor sphere formation assays in ICC cells. Data was analyzed using unpaired *t* test. N.S., no significance, *$p < 0.05$, **$p < 0.01$.

with better outcomes are urgently required. Current studies have found that low-level reactive oxygen can be an effective mitogen, which is necessary for many biological processes, such as cell survival, proliferation, angiogenesis, and metastasis [9]. Excessive reactive oxygen species metabolically produced by redox transcription factors will affect the therapeutic effect of tumor drugs and lead to drug resistance [30]. Therefore, we utilized a redox library to screen the small molecule compounds to inhibit this refractory malignancy.

In this study, eight small-molecule compounds were firstly selected as candidate anti-tumor drugs by a prelimi-

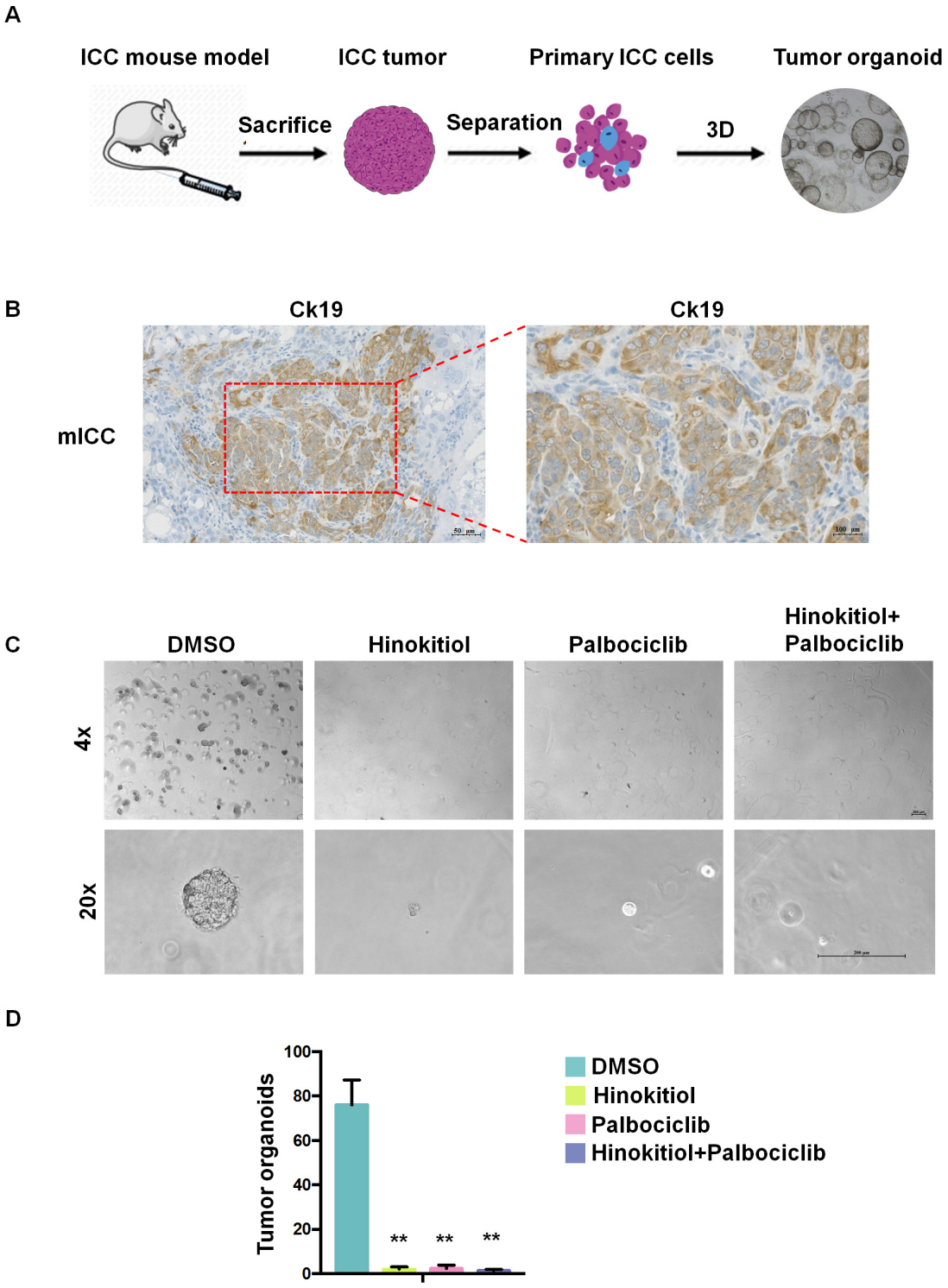

Fig. 7. Hinokitiol combined with Palbociclib significantly inhibited the formation of tumor organoids from mouse ICC models. (A) The pattern of separation of tumor organoids in mice ICC. (B) Representative IHC staining of CK19 in ICC tissues. (C) The formation of mouse ICC tumor organoids was observed after 7 days. Scale bar is 200 μm at 4$\times$ and 20$\times$ magnification. (D) The column graph of tumor organoids treated with DMSO, Hinokitiol, Palbociclib, and Hiokitiol + Palbociclib. Data was analyzed by unpaired *t* test. N.S., no significance, *$p < 0.05$, **$p < 0.01$.

nary screening stage. Among them, β-Lapachone, Thymoquinone, and N-Ethylmaleimide have been reported to induce apoptosis by blocking the cell cycle [31–33]. Furthermore, Tanshinone IIA and CAPE could inhibit tumor proliferation by inhibiting the c-Jun N-terminal kinase (JNK) signaling pathway, making the transforming growth factor

beta1/Smad (TGF-β1/Smad) signaling pathway out of balance, and targeting the epigenetics of CSC to inhibit tumor proliferation [34,35]. Ciclopirox ethanolamine and Hinokitiol have been reported to possess a remarkable antifungal effect [36,37]. However, #54 (n-Octylcaffeate) was not sold in China, so the above investigation suggests that seven other natural small molecules in the redox library could inhibit the tumor clone formation ability of ICC cells through various pathways. We further investigated that whether these small molecular inhibitors could significantly repress the CSC characteristics of ICC cells via tumor sphere formation, CSC-related marker inhibition, and organoid formation. The above experiments indicated that only Hinokitiol inhibited tumor sphere formation and suppressed the expression of some CSC-related markers *in vitro*. It has been reported that Hinokitiol inhibits epidermal growth factor-induced cell migration and signaling pathways in human cervical adenocarcinoma [38]. Zhang *et al*. [39] found that Hinokitiol can increase the sensitivity of cancer cells to radiotherapy by inhibiting homologous recombination and repair of cancer cells. Recent reports have found that Hinokitiol can induce autophagy signal transduction by downregulating the AKT/mTOR pathway, thereby inhibiting tumor growth [40,41]. In addition, Hinokitiol is also considered as a safe zinc ionophore rather than hydroxychloroquine (HCQ) for the treatment of viral infections. Moreover, Hinokitiol has been reported in skin and oral care because of its potent antiviral, anti-inflammatory, and anticancer properties [42,43]. In this study, through qRT-PCR assays and western blotting analysis screening, we found that Hinokitiol could inhibit some of the CSC characteristics of ICC cells by reducing the expression of ERK and P38, thus inhibiting tumor sphere formation.

ICC patients often exhibit high drug resistance to Palbociclib via various mechanisms, leading to an increasing proportion of CSCs and EMT [44]. In this study, we found that Hinokitiol has a better inhibitory effect when combined with Palbociclib treatment, which may play a significant role in the clinical application of ICC treatment.

We highly appreciate that ICC cells from different patients may possess different molecular mutations, such as FGFR, IDH, and BAP. The commonly used ICC cell lines may not be a good model to reflect the response of drugs in ICC patients. In our preliminary experiments, we designed an experiment to culture organoids from human ICC patients using the method of Hidetsugu Saito group [45], but in our hands, we could not successfully culture the human ICC organoids, due to the difficulty of human ICC organoid culture and the scarcity of human ICC fresh samples. Instead, we have successfully cultured the mouse ICC organoids from hydrodynamic transfection-induced mouse ICC tissues, we will consider mutating the mouse ICC organoids to screen the drugs in the future. Actually, Segatto *et al*. [46] reported that FGFR2 fusion proteins drive oncogenic transformation of liver organoids from mouse ICC tissues.

5. Conclusions

In conclusion, a natural small molecule compound, Hinokitiol, was found in a redox library that could effectively inhibit the growth of ICC cells. Our results showed that Hinokitiol can effectively inhibit tumor sphere proliferation *in vitro* by downregulating the expression of the ERK and P38 pathways. Moreover, its combination with the clinical drug, Palbociclib, showed significant anti-tumor effects in human ICC cells and mouse ICC organoids. Therefore, the study of Hinokitiol and Palbociclib provides a promising application for the treatment of patients with ICC.

Abbreviations

ICC, Intrahepatic cholangiocarcinoma; CSC, cancer stem cell; qRT-PCR, quantitative reverse-transcription polymerase chain reaction; HCC, hepatocellular carcinoma; Nrf2, nuclear factor-erythroid 2 related factor 2; APE-1/Ref-1, Apurinic-apyrimidinic endonuclease 1/redox factor 1; MAPK, Mitogen-activated protein kinase; EMT, epithelial-mesenchymal transition; JNK, c-Jun N-terminal kinase; TGF-β1/Smad, Transforming growth factor beta1/Smad; ERK, extracellular regulated protein kinases; DMSO, dimethyl sulfoxide; ROCK, Rho-associated protein kinase.

Author contributions

XLY, WY, and XTP conceived and designed the experiments; PB, CG, HY, and HC performed the experiments and analyzed the data; LW, YZ, BZ, QZ, and ZF analyzed the data.

Ethics approval and consent to participate

The institutional review board of the Beijing University of Technology approved animal experiments, code 20200311.

Acknowledgment

We would like to thank Editage (www.editage.cn) for English language editing.

Funding

The research was supported by grants from National Natural Science Foundation of China (81772617, 82173183), Great Wall Scholar Project (CIT&TCD20190311).

Conflict of interest

The authors declare no conflict of interest.

Supplementary material

Supplementary material associated with this article can be found, in the online version, at https://www.imrpress.com/journal/FBL/27/1/10.31083/j.fbl2701018.

References

[1] Rizvi S, Khan SA, Hallemeier CL, Kelley RK, Gores GJ. Cholangiocarcinoma — evolving concepts and therapeutic strategies. Nature Reviews Clinical Oncology. 2018; 15: 95–111.

[2] Esnaola NF, Meyer JE, Karachristos A, Maranki JL, Camp ER, Denlinger CS. Evaluation and management of intrahepatic and extrahepatic cholangiocarcinoma. Cancer. 2016; 122: 1349–1369.

[3] Sirica AE, Gores GJ, Groopman JD, Selaru FM, Strazzabosco M, Wei Wang X, *et al*. Intrahepatic Cholangiocarcinoma: Continuing Challenges and Translational Advances. Hepatology. 2019; 69: 1803–1815.

[4] Moeini A, Sia D, Bardeesy N, Mazzaferro V, Llovet JM. Molecular Pathogenesis and Targeted Therapies for Intrahepatic Cholangiocarcinoma. Clinical Cancer Research. 2016; 22: 291–300.

[5] Rizvi S, Gores GJ. Pathogenesis, Diagnosis, and Management of Cholangiocarcinoma. Gastroenterology. 2013; 145: 1215–1229.

[6] Zhang M, Yang H, Wan L, Wang Z, Wang H, Ge C, *et al*. Single-cell transcriptomic architecture and intercellular crosstalk of human intrahepatic cholangiocarcinoma. Journal of Hepatology. 2020; 73: 1118–1130.

[7] Kartal-Yandim M, Adan-Gokbulut A, Baran Y. Molecular mechanisms of drug resistance and its reversal in cancer. Critical Reviews in Biotechnology. 2016; 36: 716–726.

[8] Assaraf YG, Brozovic A, Gonçalves AC, Jurkovicova D, Linē A, Machuqueiro M, *et al*. The multi-factorial nature of clinical multidrug resistance in cancer. Drug Resistance Updates. 2019; 46: 100645.

[9] Polimeni M, Gazzano E. Is redox signaling a feasible target for overcoming multidrug resistance in cancer chemotherapy? Frontiers in Pharmacology. 2014; 5: 286.

[10] Cort A, Ozben T, Saso L, De Luca C, Korkina L. Redox Control of Multidrug Resistance and its Possible Modulation by Antioxidants. Oxidative Medicine and Cellular Longevity. 2016; 2016: 4251912.

[11] Di Sotto A, Di Giacomo S, Rubini E, Macone A, Gulli M, Mammola CL, *et al*. Modulation of STAT3 Signaling, Cell Redox Defenses and Cell Cycle Checkpoints by β-Caryophyllene in Cholangiocarcinoma Cells: Possible Mechanisms Accounting for Doxorubicin Chemosensitization and Chemoprevention. Cells. 2020; 9: 858.

[12] Schieber M, Chandel NS. ROS function in redox signaling and oxidative stress. Current Biology. 2014; 24: R453–R462.

[13] Haddad JJ. Oxygen homeostasis, thiol equilibrium and redox regulation of signalling transcription factors in the alveolar epithelium. Cellular Signalling. 2002; 14: 799–810.

[14] Suphim B, Prawan A, Kukongviriyapan U, Kongpetch S, Buranrat B, Kukongviriyapan V. Redox modulation and human bile duct cancer inhibition by curcumin. Food and Chemical Toxicology. 2010; 48: 2265–2272.

[15] Wang K, Jiang J, Lei Y, Zhou S, Wei Y, Huang C. Targeting Metabolic-Redox Circuits for Cancer Therapy. Trends in Biochemical Sciences. 2019; 44: 401–414.

[16] Chaiswing L, St Clair WH, St Clair DK. Redox Paradox: A Novel Approach to Therapeutics-Resistant Cancer. Antioxidants and Redox Signaling. 2018; 29: 1237–1272.

[17] Cui Q, Wang J, Assaraf YG, Ren L, Gupta P, Wei L, *et al*. Modulating ROS to overcome multidrug resistance in cancer. Drug Resistance Updates. 2018; 41: 1–25.

[18] Yang Y, Karakhanova S, Hartwig W, D'Haese JG, Philippov PP, Werner J, *et al*. Mitochondria and Mitochondrial ROS in Cancer: Novel Targets for Anticancer Therapy. Journal of Cellular Physiology. 2016; 231: 2570–2581.

[19] Sallmyr A, Fan J, Rassool FV. Genomic instability in myeloid malignancies: increased reactive oxygen species (ROS), DNA double strand breaks (DSBs) and error-prone repair. Cancer Letters. 2008; 270: 1–9.

[20] Suzuki T, Yamamoto M. Molecular basis of the Keap1-Nrf2 system. Free Radical Biology and Medicine. 2015; 88: 93–100.

[21] Shaw P, Chattopadhyay A. Nrf2-ARE signaling in cellular protection: Mechanism of action and the regulatory mechanisms. Journal of Cellular Physiology. 2020; 235: 3119–3130.

[22] Ma Q. Role of nrf2 in oxidative stress and toxicity. Annual Review of Pharmacology and Toxicology. 2013; 53: 401–426.

[23] Zhang Y, Wang J. Anticancer clinical utility of the apurinic/apyrimidinic endonuclease/redox factor-1 (APE/Ref-1). Chinese Journal of Cancer. 2010 29: 333–339.

[24] Garcia-Mayea Y, Mir C, Masson F, Paciucci R, LLeonart ME. Insights into new mechanisms and models of cancer stem cell multidrug resistance. Seminars in Cancer Biology. 2020; 60: 166–180.

[25] Wang T, Chen L, Zhao X. Prediction of Drug Combinations with a Network Embedding Method. Combinatorial Chemistry and High Throughput Screening. 2018; 21: 789–797.

[26] Song X, Liu X, Wang H, Wang J, Qiao Y, Cigliano A, *et al*. Combined CDK4/6 and Pan-mTOR Inhibition is Synergistic against Intrahepatic Cholangiocarcinoma. Clinical Cancer Research. 2019; 25: 403–413.

[27] Yamamoto M, Xin B, Watanabe K, Ooshio T, Fujii K, Chen X, *et al*. Oncogenic Determination of a Broad Spectrum of Phenotypes of Hepatocyte-Derived Mouse Liver Tumors. The American Journal of Pathology. 2017; 187: 2711–2725.

[28] Wang J, Dong M, Xu Z, Song X, Zhang S, Qiao Y, *et al*. Notch2 controls hepatocyte-derived cholangiocarcinoma formation in mice. Oncogene. 2018; 37: 3229–3242.

[29] Cillo U, Fondevila C, Donadon M, Gringeri E, Mocchegiani F, Schlitt HJ, *et al*. Surgery for cholangiocarcinoma. Liver International. 2019; 39: 143–155.

[30] Wang S, Yu G, Wang Z, Jacobson O, Lin L, Yang W, *et al*. Enhanced Antitumor Efficacy by a Cascade of Reactive Oxygen Species Generation and Drug Release. Angewandte Chemie International Edition. 2019; 58: 14758–14763.

[31] Liu Y, Kwon T, Kim JS, Chandimali N, Jin YH, Gong YX, *et al*. Peroxiredoxin V Reduces β-Lapachone-induced Apoptosis of Colon Cancer Cells. Anticancer Research. 2019; 39: 3677–3686.

[32] Mahmoud YK, Abdelrazek HMA. Cancer: Thymoquinone antioxidant/pro-oxidant effect as potential anticancer remedy. Biomedicine and Pharmacotherapy. 2019; 115: 108783.

[33] Shakhristova EV, Stepovaya EA, Rudikov EV, Novitskii VV. Oxidative Modification of Redox Proteins: Role in the Regulation of HBL-100 Cell Proliferation. Bulletin of Experimental Biology and Medicine. 2019; 167: 30–34.

[34] Feng F, Li N, Cheng P, Zhang H, Wang H, Wang Y, *et al*. Tanshinone IIA attenuates silica-induced pulmonary fibrosis via inhibition of TGF-β1-Smad signaling pathway. Biomedicine and Pharmacotherapy. 2020; 121: 109586.

[35] Kim EY, Ryu J, Kim AK. CAPE promotes TRAIL-induced apoptosis through the upregulation of TRAIL receptors via activation of p38 and suppression of JNK in SK-Hep1 hepatocellular carcinoma cells. International Journal of Oncology. 2013; 43: 1291–1300.

[36] Kang JA, Kim S, Park M, Park HJ, Kim JH, Park S, *et al*. Ciclopirox inhibits Hepatitis B Virus secretion by blocking capsid assembly. Nature Communications. 2019; 10: 2184.

[37] Domon H, Hiyoshi T, Maekawa T, Yonezawa D, Tamura H, Kawabata S, *et al*. Antibacterial activity of hinokitiol against both antibiotic-resistant and -susceptible pathogenic bacteria that predominate in the oral cavity and upper airways. Microbiology and Immunology. 2019; 63: 213–222.

[38] Wang CC, Chen BK, Chen PH, Chen LC. Hinokitiol induces cell death and inhibits epidermal growth factor-induced cell migration and signaling pathways in human cervical adenocarcinoma. Taiwanese Journal of Obstetrics and Gynecology. 2020; 59: 698–705.

[39] Zhang L, Peng Y, Uray IP, Shen J, Wang L, Peng X, *et al*. Natural product β-thujaplicin inhibits homologous recombination repair and sensitizes cancer cells to radiation therapy. DNA Repair. 2017; 60: 89–101.

[40] Zhang G, He J, Ye X, Zhu J, Hu X, Shen M, *et al*. B-Thujaplicin induces autophagic cell death, apoptosis, and cell cycle arrest through ROS-mediated Akt and p38/ERK MAPK signaling in human hepatocellular carcinoma. Cell Death and Disease. 2019; 10: 255.

[41] Xin B, Yamamoto M, Fujii K, Ooshio T, Chen X, Okada Y, *et al*. Critical role of Myc activation in mouse hepatocarcinogenesis induced by the activation of AKT and RAS pathways. Oncogene. 2017; 36: 5087–5097.

[42] Hoang BX, Han B. A possible application of hinokitiol as a natural zinc ionophore and anti-infective agent for the prevention and treatment of COVID-19 and viral infections. Medical Hypotheses. 2020; 145: 110333.

[43] Iha K, Suzuki N, Yoneda M, Takeshita T, Hirofuji T. Effect of mouth cleaning with hinokitiol-containing gel on oral malodor: a randomized, open-label pilot study. Oral Surgery, Oral Medicine, Oral Pathology and Oral Radiology. 2013; 116: 433–439.

[44] Rencuzogulları O, Yerlikaya PO, Gürkan AC, Arısan ED, Telci D. Palbociclib, a selective CDK4/6 inhibitor, restricts cell survival and epithelial-mesenchymal transition in Panc-1 and MiaPaCa-2 pancreatic cancer cells. Journal of Cellular Biochemistry. 2020; 121: 508–523.

[45] Saito Y, Muramatsu T, Kanai Y, Ojima H, Sukeda A, Hiraoka N, *et al*. Establishment of Patient-Derived Organoids and Drug Screening for Biliary Tract Carcinoma. Cell Reports. 2019; 27: 1265–1276.e4.

[46] Cristinziano G, Porru M, Lamberti D, Buglioni S, Rollo F, Amoreo CA, *et al*. FGFR2 fusion proteins drive oncogenic transformation of mouse liver organoids towards cholangiocarcinoma. Journal of Hepatology. 2021; 75: 351–362.